MODELLING HEAT TRANSFER IN AN INTUMESCENT PAINT AND ITS EFFECT ON FIRE RESISTANCE OF ON-BOARD HYDROGEN STORAGE

Kim, Y., Makarov, D., Kashkarov, S., Joseph, P. and Molkov, V.
[1] HySAFER Centre, Ulster University, Shore Road, Newtownabbey, BT37 0QB, U.K.
y.kim@ulster.ac.uk

ABSTRACT

This paper describes a 1-D numerical model for the prediction of heat and mass transfer through an intumescent paint that is applied to an on-board high-pressure GH2 storage tank. The intumescent paint is treated as a composite system, consisting of three general components, decomposing in accordance with independent finite reaction rates. A moving mesh that is employed for a better prediction of the expansion process of the intumescent paint is based on the local changes of heat and mass. The numerical model is validated against experiments by Cagliostro et al. (1975). The overall model results are used to estimate effect of intumescent paint on fire resistance of carbon-fibre reinforced GH2 storage.

1.0 INTRODUCTION

1.1 Fire resistance rating and safety strategy for on-board GH2 storage

From a safety point of view, particular attention has to be paid when a thermally-activated pressure relief device (TPRD) is opened to release hydrogen for the prevention of catastrophic failure of on-board hydrogen tanks. The regulations, code and standards that are currently available, however, do not specify an important aspect, such as the duration of hydrogen blowdown process, maximum flame length and maximum allowable orifice diameter. Constraints placed on the flexibility of the design parameters may then lead to a potentially hazardous situations such as jet fires and pressure peaking phenomena (in confined spaces) introduced by hydrogen releases from TPRDs [2]. One of the potential solutions to resolve these hazardous situations is the reduction of mass flow rates by reducing the TPRD diameter. This in turn results in the reduction of jet fire length, separation distance and peaking of overpressure in a confined space.

A carbon-fibre reinforced composite tank with plastic liner (type 4 tank) can only withstand a fire up to about 6-12 minutes before a catastrophic failure [3-5]. In order to reduce the TPRD diameter, a longer fire resistance rating (FRR) must be provided. This will ensure that there is sufficient time for the hydrogen blowdown from a relatively small TPRD orifice. Indeed, the increase of FRR of hydrogen on-board tanks to 30 minutes would allow using TPRD with a diameter of 1 mm, which would then result in a maximum flame length of 3 m at a storage pressure of 35 MPa [2]. In this context, we would expect that the destruction of an enclosure like a garage due to the pressure peaking phenomenon will be excluded, and that the separation distances, that are proportional to the TPRD diameter, will be reduced resulting from an increased fire resistance rating coupled to a smaller TPRD diameter.

1.2 Intumescent paint and application into hydrogen on-board storage tank

The most straightforward solution to increase FRR is to provide thermal protection to the tank in the event of a fire. One promising method, which is applied in the current study, is to apply a fire retardant intumescent coating on the surface of the on-board hydrogen storage tank with a view to providing the necessary thermal resistance. Several related reports, concerning the performance of intumescent paint coating on the fibre-reinforced polymer composites, are given in the literature [6-10]. Kandola et al.

[6] investigated the performance of intumescent coating on glass fibre-reinforced epoxy composites. The time-to-ignition was delayed about 4 times and the occurrence of the peak heat release rate was reduced about 3 times at an external heat flux of 25 kW/m^2, for the paint-protected composite. They concluded that the intumescent coating provided a significant improvement in the overall fire performance of the composite material. Quang Dao et al. [7] compared the thermal performance of an ablative elastomer and that of an intumescent coating painted on an epoxy resin/carbon fibre composite. Similar to [6], the time-to-ignition was significantly delayed (from 33 ± 3 s to 496 ± 5 s at the external heat flux of 75 kW/m^2) and the critical heat flux is also enhanced (from 14 kW/m^2 to 30 kW/m^2 s at an external heat flux of 75 kW/m^2) for the paint-protected composite. Also, results showed that the ablative elastomer exhibited a better fire protective performance at low temperatures, whereas the intumescent coating showed a better performance at high temperatures. Zhuge et al. [8] developed a carbon nano-fibre based nano-paper and compared its flame retardant efficiency by thermogravimetric analysis and cone calorimeter tests. They found that the nano-paper acted as a thermal barrier, like a protective char layer. The performance of this thin nano-paper as thermal resistance was significant considering its thickness (back-side temperature of substrate was reduced about 10 % with nano-paper thickness of 10 nm), but commercialization of such an approach is still questionable. Gambone and Wong [9] experimentally tested the thermal resistance performance of a sprayed ceramic insulating material coated on the natural gas storage tank. Webster [10] tested thermal performance of intumescent paints coated on the hydrogen storage tanks. Results from both studies showed that the intumescent paint considerably increased the FRR of the storage tanks (for instance, temperature on inner surface of tank is just increased about 50 ^{o}C for 10 minutes when surface temperature of tank is quickly reached and stabilized at 800 ^{o}C). Generally, almost all of the previous works reported in the literature revealed significant improvements in thermal resistance of the base materials by applying a coating of an intumescent paint. However, except for work done by Gambone and Wong [9] and Webster [10], there is no detailed investigation reported in terms of the FRR of on-board hydrogen storage tank enhanced by an intumescent paint.

The aim of the present work is to estimate the effect of an intumescent paint on fire resistance of carbon-fibre reinforced GH2 storage by a 1D numerical simulation.

2.0 PROLBEM FORMULATION

2.1 Simplification of the problem and intumescence process

The problem considers a bonfire test of a carbon-fibre reinforced polymer (CFRP) GH2 storage tank with a high-density polyethylene (HDPE) liner which is thermally protected by an intumescent paint (Fig. 1). To simplify the problem formulation and reduce CFD resources the real bonfire test was simulated in three stages:

- first 3D bonfire test of a bare tank was simulated to obtain the surface temperature and heat flux distribution on the tank surface with time using a fixed mesh;
- then a boundary condition was formulated by using obtained surface temperature and heat flux at the bottom surface of the tank and above the centre of the burner (see 2.3);
- finally a 1D problem of intumescent paint coated tank was solved by applying a boundary condition, which is based on 3D bonfire, with dynamic mesh for modelling intumescent paint swelling.

Although the process of intumescent action depends on its components, and that there are diverse types of intumescent paints, the general physico-chemical processes, especially, from a chemical perspective can be described as follows.

Intumescence is a versatile method for providing resistance to fire to a variety of materials. When heated beyond a critical temperature, an intumescent material begins to swell and then to expand forming an insulative coating that limits heat transfer. However, the actual physico-chemical processes

behind the production of the intumescent char can be very complex. Generally, the intumescent material is multi-component system, essentially consisting of a char former (e.g. pentaerythritol), an acidic component (e.g. ammonium polyphosphate) and a spumific/blowing agent (e.g. melamine). Upon heating, the acidic component will react with the char former, thus producing a carbonaceous char, which will be subsequently blown-up by relatively incombustible gaseous products from the decomposing spumific agent. Whilst as a gross estimation, the three components can be taken as to be acting almost independently, it is often the case that the individual steps overlap, thus making the whole process much more complex to predict and model. Since its inception, intumescent systems have greatly evolved, both in terms of their chemical nature and composition, and have expanded rapidly into a vast variety of formulations, each tailored for a wide collection of material substrates.

The detailed assessment of the intumescent coatings performance is almost impossible due to the underlying complicated physico-chemical processes. Thus, numerical model in this study follows a simplified representation of chemical and physical processes in the intumescent paint. Figure 1 schematically shows the intumescence process as applied in this study. When the intumescent paint is irradiated with heat, the acid source first decomposes to a mineral acid, which then takes part in the charring reaction to generate a carbon-rich char. In tandem with charring reaction, the blowing agent decomposes to form gaseous products. A fraction of the gases from the blowing agent is assumed to be involved in the swelling process of coating, whereas the rest is instantaneously released into ambient atmosphere. As temperature increases, the carbon char gets oxidized thereby finally leaving a layer of solid, multi-cellular char structure.

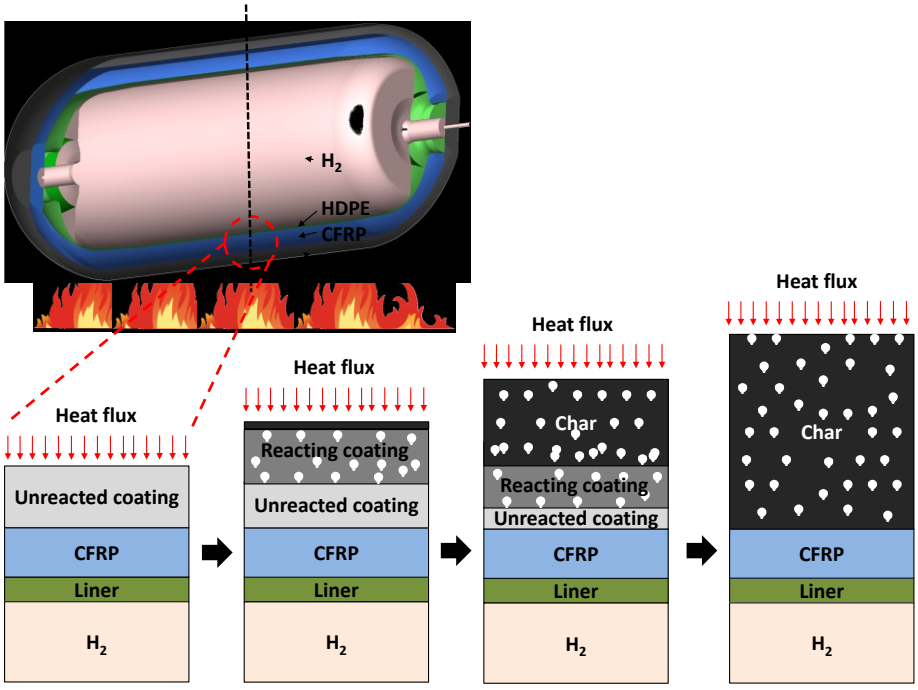

Figure 1. Schematic description for the problem simplification and physical process of the intumescence behaviour

2.2 The governing equations

The mass and energy conservations are only solved for the intumescence process here, and are based on [11-15]. It is assumed that the paint consists of three components, an inorganic acid source (S_1), a

blowing agent (S_2) and a charring material (S_3), with the initial mass fractions of $Y_{1.0}$, $Y_{2,0}$ and $Y_{3,0}$, respectively. These three components are assumed to undergo three independent reactions in accordance with the three reaction rates, K_1, K_2 and K_3. G_1, G_2 and G_3 are the corresponding gas species and C is the charred solid residue.

$$S_1 \xrightarrow{k_1} G_1, S_2 \xrightarrow{k_2} G_2, S_3 \xrightarrow{k_3} \nu_C G_C + \nu_V G_3, \tag{1}$$

$$k_j = A_i \exp\left(-\frac{E_j}{RT}\right), j = 1, 2, 3, \tag{2}$$

$$\frac{\partial Y_1}{\partial t} = -K_1 Y_1, \frac{\partial Y_2}{\partial t} = -K_2 {Y_2}^2, \frac{\partial Y_3}{\partial t} = -K_3 Y_3, \frac{\partial Y_C}{\partial t} = \nu_3 K_3 Y_3. \tag{3}$$

The total mass of the condensed phase species, m_s, are the sum of unreacted solid masses, including the char residue generated, and the rest of the mass losses are taken to be proportional to the total mass of the gaseous species formed, m_g. Here, $m_{0,s}$ is initial mass of coating.

$$\frac{\partial m_s}{\partial t} = -\frac{\partial m_g}{\partial t} = \sum_j \frac{\partial m_j}{\partial t} + \frac{\partial m_C}{\partial t}, \tag{4}$$

$$m_s = m_{0,s}(Y_1 + Y_2 + Y_3 + Y_C), m_g = m_{0,s} - m_s. \tag{5}$$

The mass flow rate per unit area of the travelling gas is calculated for taking into account the effect of convective heat transfer in coating.

$$\dot{m}_g = \frac{1}{A_s}\frac{\partial m_g}{\partial t} - \frac{\partial(\varepsilon \Delta x \rho_g)}{\partial t}. \tag{6}$$

Generated gases of G_1 and G_3 are assumed to leave paint instantaneously, however, some of G_2 is taken to be trapped in the paint and is assumed to participate in an expansion process. Here the amount of trapped gas is determined by an empirical parameter, the trapped gas ratio, β (in this study, β is taken to be 1). Although there is gas generation and its transport, it is assumed that the pressure in the paint is constant for the purpose of model simplification. The expansion rate (Eq. 7) is obtained from the ideal gas law, where the partial pressure of G_2 is assumed to be the atmospheric pressure. Although the empirical parameter, β, can adjust the expansion ratio, an expansion factor, E, is introduced to limit the maximum volume expansion in order to fit the measured final thickness (in this study, E=5) similar to [11-12].

$$\frac{\partial x}{\partial t} = \frac{\beta R}{A_s P_0 W_g}\left(T\frac{\partial m_2}{\partial t}\right), \quad (\Delta x \le E\Delta x_0), \tag{7}$$

$$\rho_g = \frac{W_g P_0}{RT}. \tag{8}$$

By assuming the thermal equilibrium condition, energy equation considers change in the internal energy of the coating driven by conduction, convection and radiation through intumescent paint and by the heat sink from the thermal decomposition.

$$\left(m_s c_{p,s} + m_g c_{p,g}\right)\frac{\partial T}{\partial t} + c_{p,g} T \frac{\partial m_g}{\partial t} + c_{p,s} T \frac{\partial m_s}{\partial t} = \frac{\partial}{\partial x}\left(\lambda^* \frac{\partial T}{\partial x}\right) - c_{p,g} \frac{\partial\left(\dot{m}_g T\right)}{\partial x} - \sum_j \left(H_j \frac{\partial m_j}{\partial t}\right). \quad (9)$$

Following from [16], the expanded intumescent char is treated as a porous material, with uniform distribution and sized- pores, thus allowing us to use a 1D thermal resistance network as an effective thermal conductivity medium (Eq. 10). Here, The porosity, ε, is calculated by total volume of coating, x, and volume of condensed phase, x_s. Volume of condensed phase is calculated by mass of condensed phase. Thermal conductivity of gas, λ_g, consists of pure gas conductivity, λ_{cond} [17] and contribution of radiation, λ_{rad} [15]. λ_{rad} is the function of pore diameter, d, in the intumescent paint, which is determined by Eq. 13.

$$\lambda^* = \lambda_s \frac{\lambda_g \varepsilon^{2/3} + \lambda_s (1-\varepsilon^{2/3})}{\lambda_g (\varepsilon^{2/3} - \varepsilon) + \lambda_s (1 - \varepsilon^{2/3} + \varepsilon)}, \lambda_g = \lambda_{cond} + \lambda_{rad},$$
$$\lambda_{cond} = 4.815 \times 10^{-7} T^{0.717}, \lambda_{rad} = \frac{2}{3} \times 4 de \sigma T^3, \quad (10)$$

$$\varepsilon = \frac{x - x_s}{x}, \quad (11)$$

$$x_s = x_{0,s}(1-\varepsilon_0)\frac{m_s}{m_{0,s}}, \quad (12)$$

$$d = d_0 + (d_{\max} - d_0)\left(1 - \frac{Y_2}{Y_{0,2}}\right)\frac{Y_3 + Y_C}{Y_{0,3}}. \quad (13)$$

Kinetic constants and physical properties of coating and thermal properties of tank are taken from [11] and [18] respectively.

2.3 Initial and boundary conditions

In order to apply the thermal condition of the bonfire test to this study, the total heat transfer coefficient, h_{tot}, as a function of the temperature on the tank surface, T_{wall}, is derived from the 3D bonfire simulation of bare tank in premixed methane-air burner bonfire according to GTR 2013 protocol using eddy-dissipation combustion model and DO radiation model

$$h_{tot} = (T_{Fire} - T_{wall}) / q'' \quad (14)$$

Here, the temperature of the fire, T_{fire}, is assumed as 1830 K (temperature in a near-wall control volume), the surface net heat flux on bare tank, q'', and surface temperature on bare tank, T_{wall}, are obtained from the 3D simulation.

Figure 2(a) shows the applied T_{wall}-dependent h_{tot} and Figure 2(b) shows validation of 1D simulation according to the simplified problem formulation against the 3D simulation of bonfire with conjugate heat transfer. When we look at the heat flux over the time, 1D simulation, which employed h_{tot}, clearly follows the 3D simulation. However, 1D simulation starts to over-predict the temperature on the tank surface as compared to the 3D simulation around 800 s. This could be attributed to the 3D effects, constant ambient temperature (T_{fire}), discretization method and accumulation of numerical errors, etc. As we are interested in FRR of tank, we would accept it from safety point of view and leave it as a

larger safety margin. Conjugate heat transfer and the impermeability condition are applied to: (1) interface between coating and CFRP (i - coating, j – CFRP); (2) interface between CFRP and liner (i – CFRP, j - liner); (3) interface between liner and hydrogen gas (i - liner, j – hydrogen):

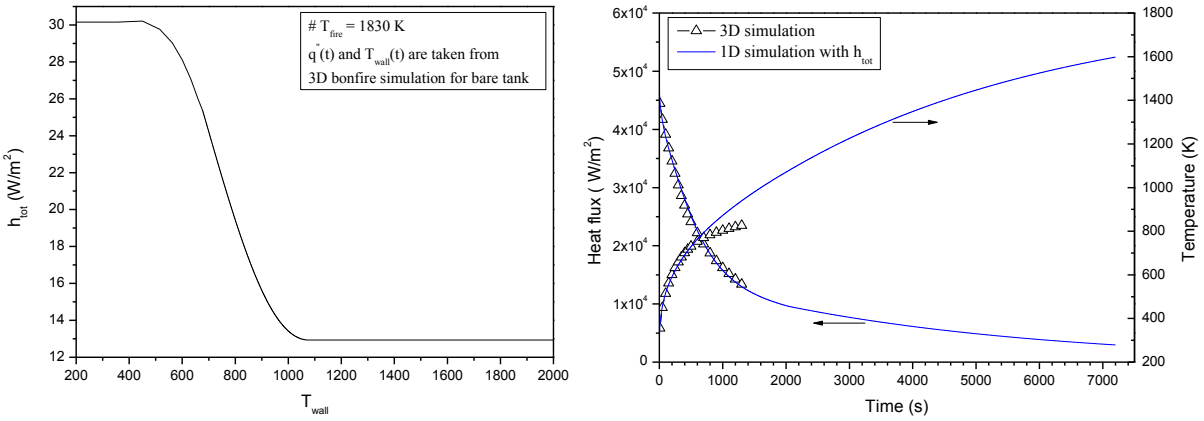

(a) (b)

Figure 2. (a) The total heat transfer coefficient as a function of the temperature on the surface of bare tank, and (b) comparison of bare tank surface temperature and net heat flux obtained in simplified 1D simulations against those for 3D simulations

$$T_i = T_j,\ \lambda_i \frac{\partial T_i}{\partial x} = \lambda_j \frac{\partial T_j}{\partial x}. \tag{15}$$

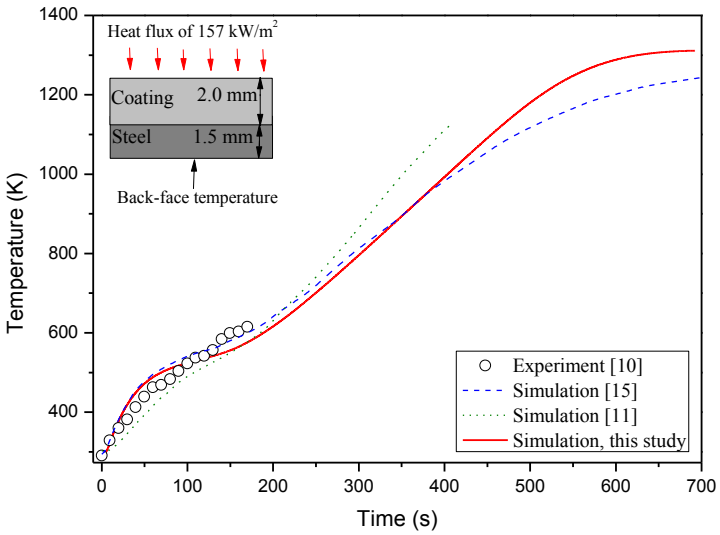

Figure 3. Validation of intumescent paint model against the cone calorimeter experiment [1] and comparison with simulations [15] and [11]

3 RESULTS AND DISCUSSION

3.1 Intumescent paint model validation

The model validation was carried out against the experimental work [1], where steel plate with thickness of 1.5 mm was thermally protected by an intumescent paint with thickness of 2.0 mm, and was subsequently exposed to a heat flux of 157 kW/m^2 (see Fig. 3). Figure 3 shows back-face temperature of the steel plate. Here, the experimental measurements (open circles) are taken from experiment [1], and the green coloured dotted line, blue coloured dash line and the red coloured thick line correspond to simulation results in [15], [11] and in the current study respectively. Although the experimental curve only shows back-side temperature up to 180 s, it can be seen that current simulation predicts back-face temperature well.

3.2 Heat transfer through the intumescent paint applied to the on-board high-pressure GH2 storage

Figure 4 shows the heat flux and temperature on the surface of hydrogen storage tank with and without intumescent paint with respect to time. Here, the open triangles and dotted line corresponds to the 3D and 1D simulation for bare tank respectively, and the green, red and violet lines stand for the 1D simulation for intumescent paint protected tank, the paint thicknesses are 10.0, 13.5 and 16.5 mm respectively. Note that, hereafter, all the results of 3D simulation for the bare tank (open triangles) are limited in time due to the fact that a catastrophic failure of a bare tank would be expected before 20 minutes [3-5]. As expected, heat flux on the coating is quickly reduced (up to the order of magnitude) with respect to time as compared to that on the surface of the bare tank. Since the char layer formed on the intumescent paint is a thermal insulator it delays heat propagation through the paint causing quick heat accumulation and temperature rise close to the coating surface. High surface temperature in turn induces the drop of the surface heat flux in case of the intumescent paint protected tank, thus resulting in lesser influx of thermal energy through the tank wall thickness including paint, CFRP and liner. The heat fluxes on the intumescent paint surface are nearly identical for different intumescent paint thicknesses, and difference in surface temperatures is barely visible on the graphs and can be taken as negligible.

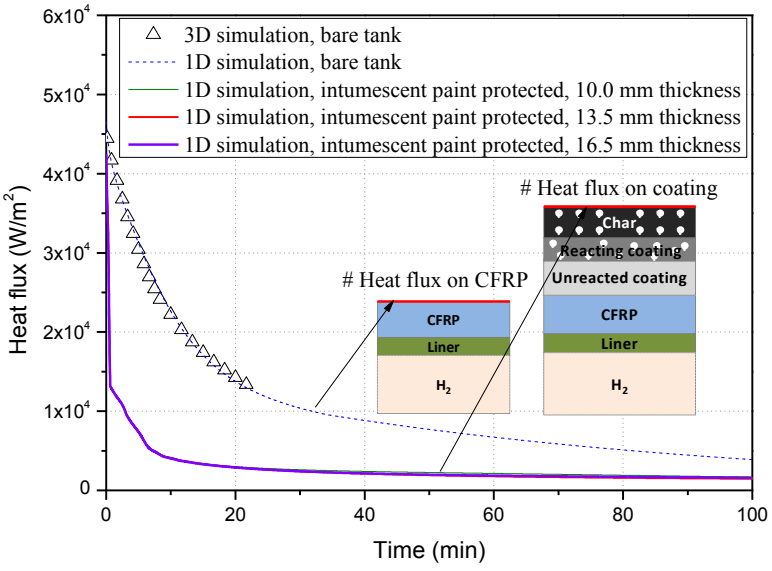

a)

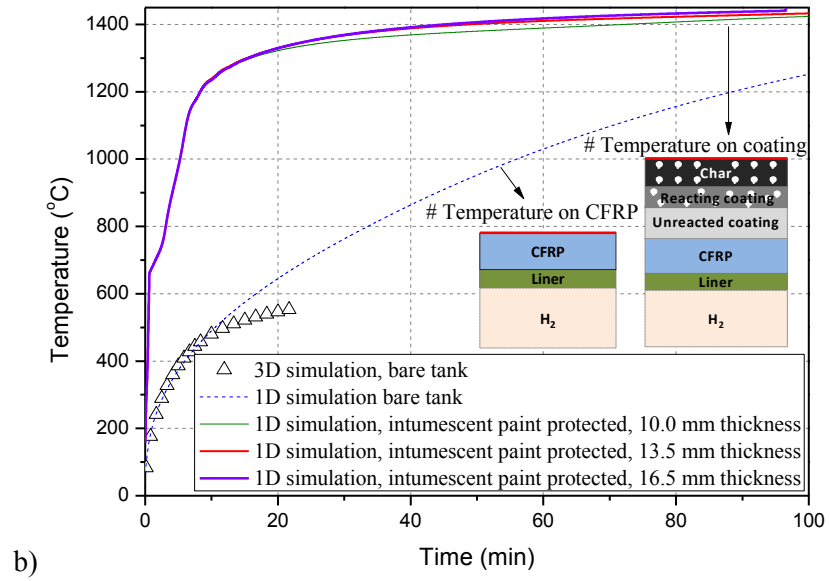

b)

Figure 4. Comparison of (a) the heat flux and (b) temperature on the surface of hydrogen storage tank with and without the intumescent paint

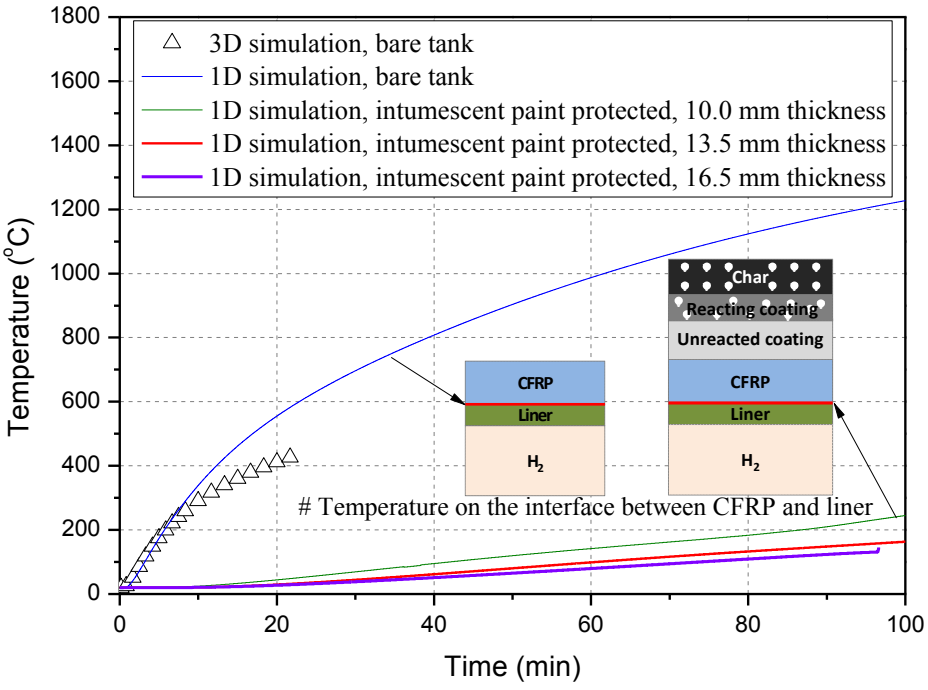

Figure 5. Comparison of temperature on the interface between CFRP and liner with and without intumescent paint

The temperature on the interface between the CFRP and liner, with and without intumescent paint, is shown in Fig. 5. When the intumescent paint is not applied, temperature rapidly increases in a short time interval. On the contrary, when the intumescent paint with thicknesses of 10.0, 13.5 and 16.5 mm is applied, the temperature is almost stagnant until 7, 13, 15 minutes, respectively. In general, it was reported that the decomposition of the epoxy resin in CFRP occurs around 350~360 °C (620~630 K)

[19-10]. Thus, the whole resin in the bare tank (open triangle and blue dotted line), without thermal protection, will almost completely degrade before 15 minutes. However, when intumescent paint is applied on the tank, the resin is expected to last in the CFRP matrix up to 2 hours.

3.3 Effect of intumescent paint on fire resistance

Figure 6 shows a comparison of the fire resistance ratings (FRR) of the bare tank and the intumescent paint-protected tank, as a function of the critical temperature of the polymer matrix. In both cases, the FRR is determined based on following assumptions:

(1) CFRP loses its mechanical strength (load bearing ability) when the epoxy resin of the CFRP reaches its critical temperature (T_c). (2) Tank failure takes place when the CFRP loses mechanical strength in the range of thickness of about 56 % from the tank surface.

The blue, pink and black dotted lines stand for the 3D bonfire simulations for the bare tank exposed to 78, 168 and 370 kW HRR, respectively. Figure 6 shows that the FRR is significantly improved when a coating is applied. For instance, if we assume that the critical temperature, T_c, is the glass transition temperature, T_g, of resin in CFRP which is around 120 ^oC [21], then the bare tank when subjected to all three HRR's is unable to withstand them for about10 minutes, whereas, the tank protected by coatings with thicknesses of 10.0, 13.5 and 16.5 mm is able to resist the heat fluxes for 49, 70 and 91 minutes, respectively. This essentially means that we can provide about 1 hour self-evacuation time for the occupants of a vehicle in the event of a fire by applying about 13.5 mm thickness of intumescent coating on the storage tank. Moreover, following from [22], a 13.5 mm thickness coating allows us to use a TPRD with 0.65 mm diameter, resulting in flame length up to 1.7 m (5 kg hydrogen storage, blowdown from 350 to 1 bar). Under the same conditions, flame length is up to about 13 m long when using typical TPRD diameter 5 mm. As a result, separation distance can be significantly reduced by introducing adequate thermal protection and a TPRD with a smaller diameter.

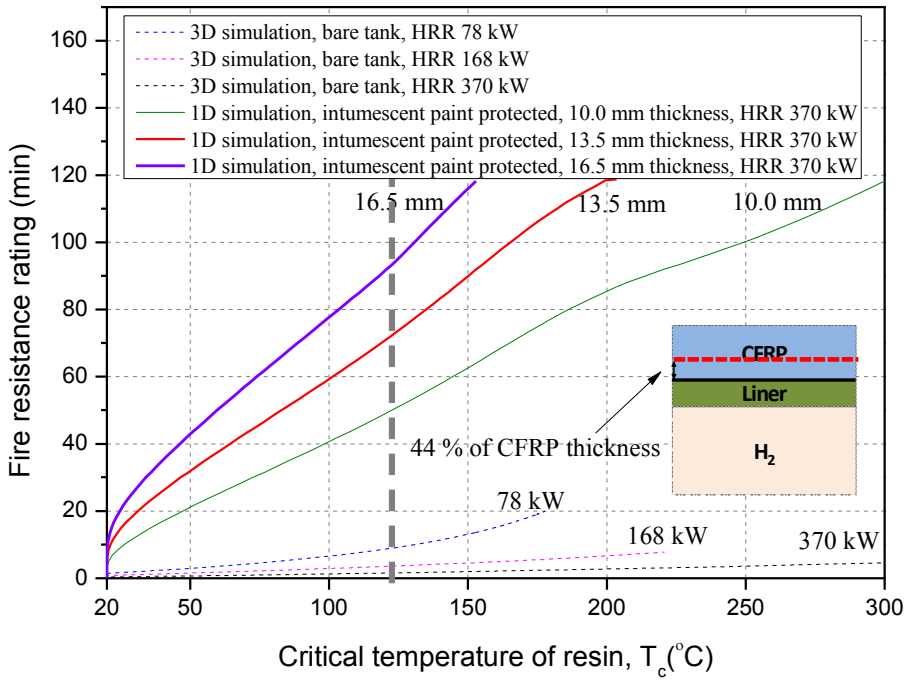

Figure 6. Comparison of fire resistance ratings of bare and intumescent paint protected tank as a function of the critical temperature

4.0 CONCLUSIONS

A 1-D numerical intumescent paint model is introduced and validated against the experiments by Cagliostro et al. (1975) showing good agreement with experimental data. The model is then applied to simulate bonfire performance of high-pressure CFRP hydrogen storage tank thermally protected by an intumescent paint. Heat flux depending on surface temperature and total heat transfer coefficient, accounting both convective and radiative heat transfer, is obtained from 3D bonfire test simulation of a bare tank and used as a boundary condition in this study. Results show a significant improvement of the tank wall thermal resistance when the intumescent paint is applied. Intumescent paint protection with thicknesses 10.0, 13.5 and 16.5 mm provided 49, 70 and 91 minutes of fire resistance rating when the T_c is the T_g of the resin in the CFRP is 120 ^oC. This is increase of 30, 40 and 55 times compare to fire resistance rating of the same but bare tank without intumescent paint protection. Conclusion is drawn that thermal protection could be an effective way to increase fire resistance and provide reduced TPRD diameter thus decreasing hazards associated with high-pressure on-board hydrogen storage.

5.0 ACKNOWLEDGEMENTS

This research was funded by the Engineering and Physical Sciences Research Council (EPSRC) U. K. (EPSRC grant number: EP/K021109/1).

REFERENCES

1. Cagliostro, D. E., Riccitiello, R and Schartel, B., Intumescent Coating Modelling, *J Fire Flammability* **6**, 1975, pp. 205–220.
2. Molkov, V., Fundamentals of Hydrogen Safety Engineering, 2012, Ventus Publishing ApS.
3. Zalosh, R. and Weyandt, N., Hydrogen Fuel Tank Fire Exposure Burst Test, *SAE Paper*, 2005, 2005-01-1886.
4. Zalosh, R., Blast Waves and Fireballs Generated by Hydrogen Fuel Tank Rupture during Fire Exposure, *5th International Seminar on Fire and Explosion Hazards*, 23-27 April, 2007, Edinburgh, UK.
5. Ruban, S., Heudier, L., Jamois, D., Proust, C., Bustamante-Valencia, L., Jallais, S., Kremer-Knobloch, K., Maugy, C. and Villalonga, S., Fire Risk on High-pressure Full Composite Cylinders for Automotive Applications. *Int. J. Hydrog. Energy* **37**, 2012, pp. 17630–17638.
6. Kandola, B. K., Bhatti, W. and Kandare, E., A Comparative Study on the Efficacy of Varied Surface Catings in Fireproofing Galass/Epoxy Composites, *Polymer Degradation and Stability*, **97**, 2012, pp. 2418–2427.
7. Quang Dao, D., Luche, J., Rogaume, T., Richard, F, Bustamante-Valencia, L. and Ruban, S., Fire Protective Performance of Intumescent Paint and Ablative Elastomer Used for High Pressure Hydrogen Composite Cylinder, *Proceedings of the 11th International Symposium on Fire Safety Science*, 2014, Christchurch, New Zealand.
8. Zhuge, J., Gou, J. Chen, R-H, Zhou, A. and Yu, Z., Fire Performance and Post-Fire Mechanical Properties of Polymer Composites Coated with Hybrid Carbon Nanofiber Paper, *Journal of Applied Polymer Science*, **124**, 2011, pp. 37–48.
9. Gambone, L. and Wong, J., Fire Protection Strategy for Compressed Hydrogen-Powered Vehicles, *2nd International Conference on Hydrogen Safety*, 2007, San Sebastian, Spain.
10. Webster, C., Localized Fire Protection Assessment for Vehicle Compressed Hydrogen Containers, 2010, Final No. DOT HS 811 303.
11. Di Blasi, C. and Branca, C., Mathematical Model for the Nonsteady Decomposition of Intumescent Coatings, *AIChEJ.*, **47**(10), 2001, pp. 2359–2370.

12. Di Blasi, C., Modeling the Effects of High Radiative Fluxes on Intumescent Material Decomposition, *J. Anal. Appl. Pyrolysis*, **8**, 2004, pp. 721–737.
13. Zhang, Y., Wang, Y. C., Bailey, C. G. and Taylor, P., Global Modelling of Fire Protection Performance of an Intumescent Coating under Different Furnace Fire Conditions, *Journal of Fire Sciences*, **31**(1), 2012, pp. 51–72.
14. Zhang, Y., Wang, Y. C., Bailey, C. G. and Taylor, P., Global Modelling of Fire Protection Performance of an Intumescent Coating under Different Cone Calorimeter Heating Conditions, *Fire Safety Journal*, **50**, 2012, pp. 51–62.
15. Yuan, J.F., Intumescent Coating Performance on Steel Structures under Realistic Fire Conditions, 2009, University of Manchester, Manchester.
16. Russell, H. W., Principles of Heat Flow in Porous Insulators, *J. Am. Ceram. Soc*., 1935, **99**. 18, 1-5.
17. Di Blasi, C., Heat, Momentum and Mass Transfer through a Shrinking Biomass Particle Exposed to Thermal Radiation, *Chem. Eng. Sci*., **51**, 1996, pp. 1121-1132.
18. Starnes, M. A., Carino, N. J. and Kausel, E. A., Preliminary Thermography Studies for Quality Control of Concrete Structures Strengthened with Fiber-reinforced Polymer Composites, *J. Mater. Civ. Eng*., **15**, 2003, pp. 266-273.
19. Pan, C.T. and Hocheng, H., Evaluation of Anisotropic Thermal Conductivity for Unidirectional FRP in Laser Machining, *Composites: Part A*, **32**, 2001, pp.1657-1667.
20. Merino-Pérez, J.L., Hodzic, A., Merson, E. and Ayvar-Soberanis, S., On the Temperatures Developed in CFRP Drilling using Uncoated WC-Co Tools Part II: Nanomechanical Study of Thermally Aged CFRP Composites, *Composite Structures*, **123**, 2015, pp. 30-34.
21. Enhanced Design Requirements and Testing Procedures for Composite Cylinders Intended for the Safe Storage of Hydrogen, HyCOMP, (http://www.hycomp.eu/).
22. H2FC Sage Framework, (http://h2fc.eu/sageserver).